2012

Development of a high sensitive automatic setup for screening of microcystins in surface waters by employing a LED-based photometric detector

SENSORS AND ACTUATORS B-CHEMICAL, LAUSANNE, v. 161, n. 1, pp. 422-428, JAN 3, 2012
http://www.producao.usp.br/handle/BDPI/42210

Sensors and Actuators B 161 (2012) 422–428

Contents lists available at SciVerse ScienceDirect

Sensors and Actuators B: Chemical

journal homepage: www.elsevier.com/locate/snb

Development of a high sensitive automatic setup for screening of microcystins in surface waters by employing a LED-based photometric detector

Gláucia P. Vieira, Sheila R.W. Perdigão, Marli F. Fiore, Boaventura F. Reis*

Centro de Energia Nuclear na Agricultura, Universidade de São Paulo, Av. Centenário, 303 – São Dimas, 13400 970 Piracicaba – SP, Brazil

ARTICLE INFO

Article history:
Received 27 March 2011
Received in revised form 17 October 2011
Accepted 22 October 2011
Available online 29 October 2011

Keywords:
Microcystins
Enzyme-linked immunosorbent assay
Surface waters
LED-based photometer
Automation
Multicommuted flow analysis

ABSTRACT

In this manuscript, an automatic setup for screening of microcystins in surface waters by employing photometric detection is described. Microcystins are toxins delivered by cyanobacteria within an aquatic environment, which have been considered strongly poisonous for humans. For that reason, the World Health Organization (WHO) has proposed a provisional guideline value for drinking water of 1 $\mu g\,L^{-1}$. In this work, we developed an automated equipment setup, which allows the screening of water for concentration of microcystins below 0.1 $\mu g\,L^{-1}$. The photometric method was based on the enzyme-linked immunosorbent assay (ELISA) and the analytical signal was monitored at 458 nm using a homemade LED-based photometer. The proposed system was employed for the detection of microcystins in rivers and lakes waters. Accuracy was assessed by processing samples using a reference method and applying the paired *t*-test between results. No significant difference at the 95% confidence level was observed. Other useful features including a linear response ranging from 0.05 up to 2.00 $\mu g\,L^{-1}$ ($R^2 = 0.999$) and a detection limit of 0.03 $\mu g\,L^{-1}$ microcystins were achieved.

1. Introduction

Cyanobacteria thrive in the presence of sunlight and high temperatures, especially in polluted waters that are rich in nutrients [1]. Microcystins are cyanobacterial secondary metabolites delivered in water, which have been characterized as strong hepatotoxins [2–7]. The contamination of drinking water by microcystins has been suggested as a risk factor for cancer [1,4,6,7]. Cyanobacterial toxin poisoning in animals has been reported around the world, while human poisoning occurred in Australia after the exposure of individuals to contaminated drinking water [1]. Human illness and death associated with microcystin toxicity occurred among dialysis patients during 1996 in Caruaru, Brazil [1,8]. These papers showed that there is an awareness concerning the risk that aquatic organism, domestic animals and humans can be poisoned by microcystins delivered in water by the cyanobacteria [1,3,9–13]. In response, the World Health Organization (WHO) has suggested a provisional guideline value of 1 $\mu g\,L^{-1}$ microcystins in drinking water [14].

Microcystins have been determined in water by employing different separation strategies associated with several detection techniques, such as ultra-performance liquid chromatography [2], capillary electrophoresis [5], spectrophotometry [3,8,12], surface plasmon resonance immunobiosensor [15], quantum dots exploiting the photoluminescence quenching effect [16], extraction using cloud point and ionic liquid [17], and on-line microsolid-phase extraction–capillary liquid chromatography [18]. Nevertheless, the preferred method has predominantly been liquid chromatography coupled to mass spectrometry [2,10–12,14,17,18].

The ELISA (enzyme linked immunosorbent assay) method of screening for microcystins has been widely used [3,8,12,19,20], since it presents such useful features as sensitivity compatible with the World Health Organization guidelines [14]. Photometric detection in the visible range of the electromagnetic radiation spectrum, allows the use of an inexpensive photometer setup.

There is a consensus that any analytical method should be sufficiently sensitive to allow determination of microcystins in fresh water at concentrations lower than the WHO's provisional guidelines value [3]. In this work, we intend to face this challenge by developing a highly sensitive photometric setup for microcystin screening in fresh water using the ELISA methodology [3,8,12]. Because the volume of sample solution to be screened is about 200 μL, the setup needs to be developed considering this condition. Sequential injection analysis (SIA) [21–23], multisyringe flow injection analysis (MSFIA) [24,25], and multicommuted flow analysis (MCFA) [26–29] approaches afford facilities for developing automated analytical procedures using lower volumes of sample and reagent solution than those based on the usual flow injection analysis (FIA) [27,28]. In this work, the facilities afforded by the MCFA approach [32–34], is employed to develop a setup for microcystin

* Corresponding author. Tel.: +55 19 3429 4639; fax: +55 19 3429 4611.
E-mail address: reis@cena.usp.br (B.F. Reis).

0925-4005/$ – see front matter © 2011 Elsevier B.V. All rights reserved.
doi:10.1016/j.snb.2011.10.054

screening in surface water. A setup, including a manifold for handling sample solution and a LED-based photometer, is designed to allow three sampling runs to be performed using a sample volume of 200 μL, in such a way that low levels of microcystin could be detected.

2. Experimental

2.1. Samples and solutions

Purified water presenting electric conductivity less than 0.1 $\mu S\,cm^{-1}$ was used throughout. The glassware and plasticware were decontaminated by overnight immersion in a 20% (v/v) nitric acid solution. Afterwards, they were washed three times with water.

ELISA assay microplate kits for microcystins (Beacon Analytical Systems Inc., Portland, ME, USA), containing standard solutions with concentrations of 0, 0.1, 0.3, 0.8, 1.0 and 2.0 $\mu g\,L^{-1}$ microcystins, wells with immobilized antibody, and stopping solution, were used to test the setup, both during the system development phase and, afterwards, for water sample analysis. The handling of samples and standard solutions for color development prior to photometric detection were carried out according to the manufacturer's recommendations, thus each well contained a sample volume of 200 μL for microcystin determination.

Water samples were collected from the Piracicaba and Corumbataí rivers as well as lakes on farms around Piracicaba city. After filtration using a 0.45 μm Whatman filter to remove suspended solid, aliquots (10 mL) of each sample were centrifuged for 15 min. Afterwards, five aliquots (1.0 mL) of the supernatant were transferred to polypropylene vessels, which were maintained in a freezer at −4 °C. Before use, the vessels were equilibrated to the laboratory temperature (22 °C) using a water bath.

2.2. Apparatus

The microcomputer employed to control all steps of analysis including data acquisition was furnished with an electronic interface card PLC 711S (Advantech Inc., 38 Tesla Street, 100 Irvine, CA, USA) and a software application written in Visual Basic 6.0. The solution handling setup comprised a homemade syringe pump that was driven by a step-motor of 48 step per revolution; plastic syringe, 5.0 mm inner diameter and 50 mm long; a brass screw 5 cm long, 10 mm diameter and thread of 1.0 mm per revolution; a 161P011 pinch solenoid valve normally closed and a 161P021 pinch solenoid valve normally open (NResearch, 267 Fairfield Ave, West Caldwell, NJ, USA); a regulated power supply (12 V, 3 A) to feed the step-motor and the solenoid valves; two homemade digital interfaces [33] coupled to the output ports *A* and *B* of the PCL711 interface card to drive the step-motor, solenoid valves and LEDs; a homemade glass flow cell, 40 mm optical path long and 1.2 mm inner diameter (inner volume 46 μL); three transistors BC547.

The homemade photometer included a 5 mm diameter blue LED, λ = 458 nm (highly intense radiation beam); a 5 mm diameter infrared LED, λ = 830 nm; a photodiode OPT301 (Burr Brawn, Lake Forest, CA 92630); a precision instrumentation amplifier AD524 (Analog Devices, Lake Forest, CA 92630); a regulated power supply (−12 V, +12 V) to feed the photometer; two diodes 4007; and resistors of different values as indicated in Fig. 1. A photometer (Quick Elisa – Drake Equipment, São Paulo, BR) was used to directly monitor the microcystin in the micro-well that was included in the Beacon Analytical Systems kits.

2.3. Photometer assembling

To allow microcystin detection at concentration levels lower than 1 $\mu g\,L^{-1}$, the detection system of Fig. 1 was designed. The light sources (LED_1, LED_2) and the photodetector (Det) were coupled to the flow cell, forming a compact unit of downsized dimension. This arrangement was tailored in order to increase sensitivity, while using a small volume of sample solution. The LEDs were assembled in tandem and aligned with the glass cylinder (ge) to allow the propagation of both radiation beams through the flow cell.

A preliminary experiment showed that the solution used for microcystins determination does not absorb infrared radiation (λ = 830 nm). This feature was, therefore, used to detect the flow cell filling, which was done following the signal generated by the photometer. As shown in Fig. 1, the infrared LED was wired to control line d_0 of the Cnt_1 interface. This LED was switched ON when the microcomputer sent a TTL low level signal to line d_0. As shown in the inset A (Fig. 1), the transistors the Tr_1, Tr_2, and Tr_3 constituted three independent networks that were selected by sending TTL low-level signals to the d_1, d_2, and d_3 lines of the Cnt_1 interface. The current intensity drained through the LED_1 was controlled by handling the variable resistors wired to the base of the transistors. This feature was employed to establish three different values of potential difference (Pdf_1, Pdf_2 and Pdf_3) generated by the photometer.

The signal (mV) generated by the photodetector (Det) presented a direct relationship with the intensity of the radiation beam emitted by the LEDs, and the network constituted by the operational amplifier (OP) was arranged to allow a signal gain of five times. The data acquisition was performed using the analog-to-digital converter of the PCL711S interface, which has a 12-bit resolution. Its full scale was ±2047 mV with 0 mV in the center of scale. To allow the output signal to be varied from 0 to 4000 mV, the network constituted by the diodes D_1 and D_2 and the resistors R_4, R_5 and R_6 was used to establish a reference signal applied to the non-inverting input of the operational amplifier (OP). Diodes D_1 and D_2 and resistors R_4, R_5 afforded a stable potential difference of +682 and −679 mV, thus permitting a fine adjustment of the potential difference applied to the non-inverting input of the OP. This potential deference was used as a reference that was adjusted to allow that a 0 mV signal in the OP inverting input was shown by the last significant bit of the A/D output. Under this condition, the value of the read signal was 1 mV.

2.4. Flow system and procedure

The whole sample volume to be processed for microcystin screening after incubation with reagents was 200 μL. Aiming to improve sensitivity, a flow cell with optical pathlength of 40 mm and inner volume of 46 μL was employed and to assure better precision of results, three measurements per sample should be achieved. The instrument to handle sample and standard solutions showed in Fig. 2 was designed considering these requisites. The diagram represents them in the standby condition, and its working pattern is depicted in Table 1. When the software was run (step *A*), the microcomputer read the dark signal (Sk), which was done by maintaining both LEDs switched OFF (Fig. 1). Afterwards, step (*B*) was carried out to complete the photometer calibration task, which was performed by maintaining valves V_1 and V_2 switched OFF, while the step-motor was driven to pull the syringe piston in order to suction water to fill the flow cell. In this case, the microcomputer sent the appropriate control signals through the Cnt_1 and Cnt_2 interfaces. While the flow cell filling was in process, the infrared LED_2 was maintained ON, which was done by the microcomputer maintaining line d_0 (Cnt_1) activated. Under this condition, the signal generated by the photometer was related to the infrared radiation

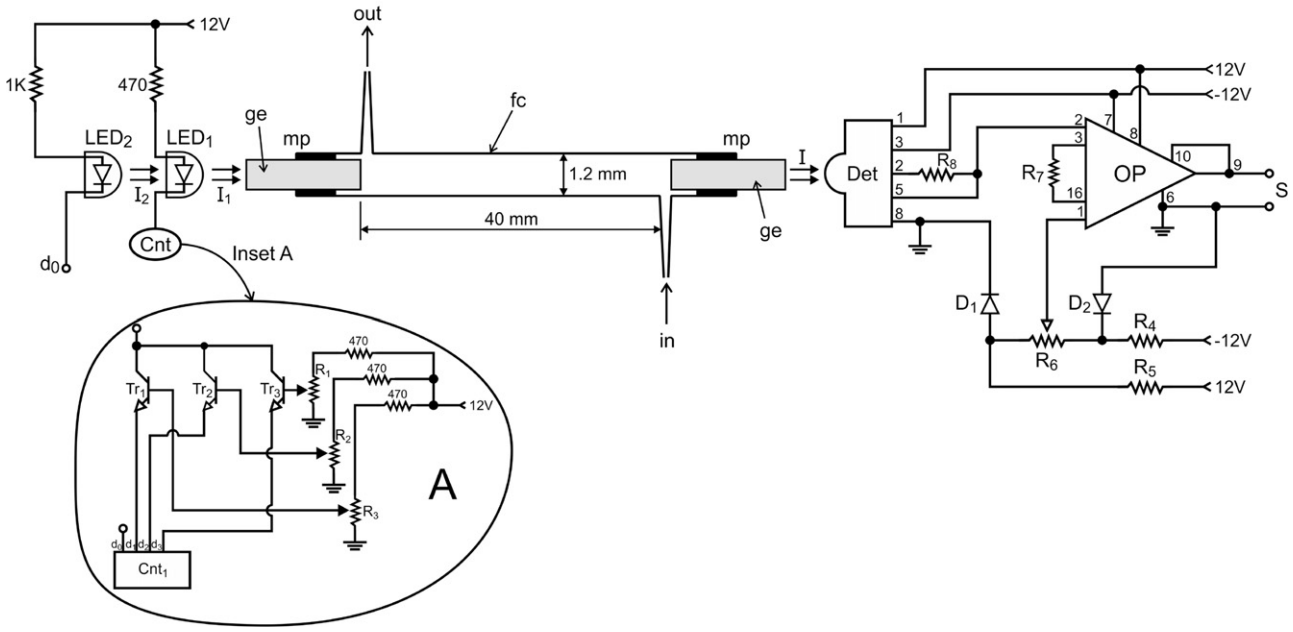

Fig. 1. Diagram of the photometer and flow cell. LED_1 = 5 mm diameter blue LED, λ = 458 nm; LED_2 = 5 mm diameter infrared LED, λ = 830 nm; I_1 and I_2 = radiation beams emitted by the LED_1 and LED_2, respectively; Cnt: control interface, inset A; ge: glass cylinders, 1.2 mm diameter and 20 mm long; mp: melted point; fc: glass tube, wall of 1.0 mm thickness; in and out: solution input and output, respectively; *I*: radiation beam coming to Det; inset A: interface to selection photometer full scale; Tr_1, Tr_2 and Tr_3: transistors BC547; Cnt_1: digital interface ULN 2803 coupled to digital output port *A* of the PCL711S interface card; d_0, d_1, d_2 and d_4: output lines of the PCL interface; Det: photodetector (OPT301); OP: AD524 operational amplifier; R_1, R_2, R_3 and R_6 = 5 kΩ ten turn variable resistors; R_4 and R_5 = 4.7 kΩ; R_7 = 10 kΩ, R_8 = 20 MΩ, resistors D_1 and D_2: diodes 4007; S: signal (mV).

beam, which was converted to digital by the PCL711 interface card. Under this condition, the signal (S) generated by the photometer was ≈400 mV. When the flow cell was filled with water, the signal monitored underwent a sudden increase, which was about two times higher than the value detected before. When this effect was detected, the microcomputer sent the control signal to switch OFF both the step-motor and the infrared LED_2. Afterwards, step (C) was carried out, the LED_1 was switched ON, and a message informing the operator to adjust the full scale values was displayed on the screen of the microcomputer. The current intensity drained through the LED_1 was controlled by handling the variable resistors wired to the base of the transistors (Fig. 1) in order to allow the establishment of three different values of potential difference (Sf_1, Sf_2 and Sf_3) generated by the photometer. To enable this calibration step, the software contained an interactive interface with the operator. When a keyboard command indicated that this task was finished, the microcomputer saved the signals (Sf_1, Sf_2 and Sf_3) as references to be used for the absorbance calculation, which were established as ≈1000, ≈2200 and ≈3500 mV. After performing steps *D* and *E*, the system was ready to carry out the analytical run. The calibration

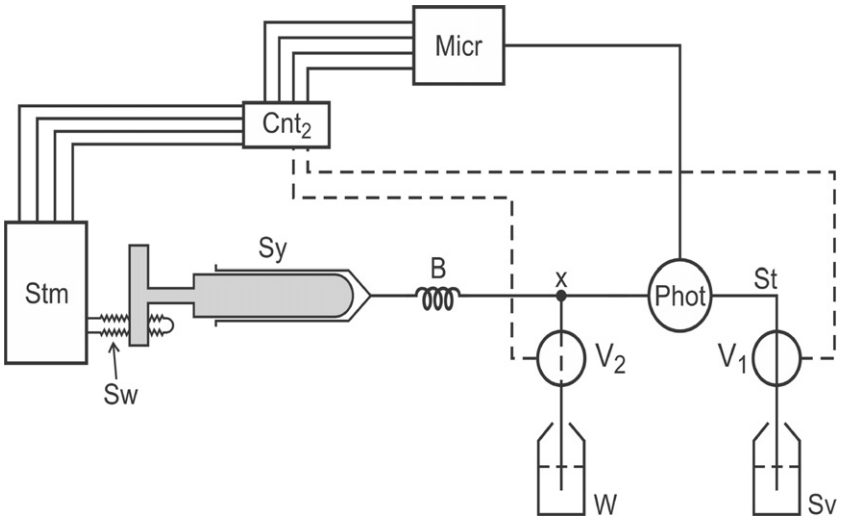

Fig. 2. Diagram of the flow system for microcystins monitoring. Stm: step-motor, 48 step per revolution; Sw: brass screw, 5 cm long, 10 mm diameter and thread of 1.0 mm per revolution; Sy: syringe, 5.0 mm inner diameter, capacity of 1.0 mL; B: holding coil, 50 cm long and 0.8 mm inner diameter; X: three-way joint device machined in acrylic; V_1 and V_2: pinch solenoid valves normally closed and open, respectively; W: waste storing vessel; Phot: LED based photometer; St: silicone sampling tube, 10 cm long and 0.5 mm inner diameter; Sv: sample vial; Micr: microcomputer; Cnt_2: digital control interface ULN 2803 coupled to the digital output port *B* of the PCL711S interface card. Continuous and interrupted lines in the valves symbols indicate that solution flowed through them while were switched OFF and ON, respectively.

Table 1
Sequence of events.

Step	Event	LED_1	LED_2	V_1	V_2	Motor	Step number
A	Reads dark signal	0[a]	0	0	0	0	–
B	Fills flow cell with water	0	1	0	0	R[b]	N_1 [c]
C	Reads blue LED reference signal	1[a]	0	0	0	0	–
D	Empts flow line	0	0	0	0	R	180
E	Empts syringe	0	0	1	1	L[b]	$180 + N_1$
F	Fills flow cell with sample	0	1	0	0	R	N_2 [c] + 48
G	Reads analytical signal	1	0	0	0	0	–
H	Inserts a new sample aliquot	1	0	0	0	R	112
I	Reads analytical signal	1	0	0	0	0	–
J	Inserts a new sample aliquot	1	0	0	0	R	112
K	Reads analytical signal	1	0	0	0	0	–
L	Empts flow cell and flow line	0	0	0	0	R	160
M	Empts syringe	0	0	1	1	L	$384 + N_2$

[a] Indicated that the corresponding device was switched OFF or ON, respectively.
[b] Indicated the step-motor rotation for right or for left, respectively.
[c] Indicated the number of control pulses sent to the step-motor up to the microcomputer sensed that flow cell was filled with water or sample solution.

was carried out 20 min after the photometer had been turned ON. The values of Sk, Sf_1, Sf_2 and Sf_3 measurements were saved to be used for the absorbance calculation.

Prior to beginning the analytical run, the microcomputer informed the operator to put the sample vial in the appropriate place to be aspirated towards the flow cell, and after a keyboard command, the steps from *F* to *K* were carried out. Step *F* was similar to step *B*, thus when the microcomputer detected that the flow cell was filled, the software carried out the activities indicated in the next step. As we can see in Table 1 (step *G*), only the LED_1 was maintained switched ON, in order to allow the monitoring of the signal related to the absorption caused by the analyte (microcystins). In steps *H* and *J*, the content of the flow cell was partially renewed by aspirating towards them a new portion of the sample solution, while in steps *I* and *K* the corresponding generated signals (S) were achieved. This strategy was implemented to allow the performing of three replicate measurements using a sample volume of 200 μL. After ending step *M*, the software control was directed to step *F*, in order to begin a new analytical run. For each standard solution processed, the measurements were carried out using the three full scale values established above, and corresponding data were saved as an ASCII file to allow further processing. While the analytical run proceeded, a graph of signal (mV) as a function of time was displayed on the microcomputer screen to allow signal visualization in real time.

The assays to find the best operational conditions were carried out using standard solutions of microcystin, prepared as indicated in the previous Section 2.1. In order to prove the effectiveness of the proposed setup, water samples of rivers and lakes were analyzed using the proposed setup together with a photometer (Quick ELISA) normally used for microcystin detection. Since the Quick ELISA setup carried out data acquisition by directly reading the solution contained in the micro-wells that were used for the reaction development, the same samples were, therefore, also read using the proposed setup, which was designed to perform three measurement replicates.

3. Results and discussion

3.1. General comments

The ELISA (enzyme linked immunosorbent assay) method [3,8,12,19,20] is based on the discoloration of the reagents solution caused by the microcystins. The reaction product of blank solution presents an intense brown color, which becomes less intense when microcystin is present in water samples or standard solutions. For analytical purposes, this effect has been monitored at 450 nm, thereby allowing the photometer included in the proposed setup to use as a radiation source a blue LED that presented a light emitting band with a maximum of around 458 nm.

3.2. The flow system and control performance

High sensitivity was an essential condition to attain low limit of detection that was the mail focus of the present work. The use of a flow cell with long optical length would have been an appropriate choice, nevertheless the little volume of sample solution (200 μL) and the intensity of the radiation beam could impair the needed sensitivity. In order to overcome this drawback, the photometer and the flow system depicted in Figs. 1 and 2 were designed. Since sample solution does not absorb infrared radiation ($\lambda = 830$ nm), this feature was used as a tool for controlling the volume sample solution inserted into the flow cell to carry out the measurement. Using data pointed out in Section 2 (caption of Fig. 2), we can deduce that the syringe pump delivered a solution volume of 0.41 μL per step, thus 112 steps were programmed to fill the flow cell. As depicted in Table 1, prior to beginning an analytical run, the flow cell and sampling tube (see Fig. 2) was emptied, which could cause an uncontrolled delay prior to beginning sample solution displacement towards the flow cell. To overcome this drawback, the infrared radiation beam was used to detect the filling of the flow cell. The parameter labeled as N_2 (Table 1, step *F*) was carried out several times, and its value varied between the range of 120–130 steps. After sensing that the flow cell was filled, an additional revolution (48 steps) was applied to the step-motor in order to discard the first portion (18 μL) of the sample that merged into the flow cell. Previous assays showed that using this strategy no carry-over effect was observed.

Because the flow cell was emptied prior to beginning the analytical run, small air bubbles could be retained within the flow cell's optical path, thereby hampering the measurements. Nevertheless, assays carried out by repeating several times steps *B*, *C*, *D* and *E* (Table 1) using water showed that the signal generated by the photometer presented standard deviation lower than 1%, which could be considered an insignificant variation. This result indicated that the air bubbles were not retained within the flow cell.

3.3. The full scale study

According to Mitteilungen [38] the Bouguer–Lambert–Beer's law is given by the following expression: absorbance = $\log(I_0/I)$, where I_0 is the radiant intensity incident upon absorbing layer and I is the radiant intensity transmitted by absorbing layer. The photodetector used in this work presented a direct relationship

Table 2
Effect of the selected full scale.

Assay	Full scale (mV)	Range ($\mu g\,L^{-1}$)	Linear equation	R^2	LD[b] ($\mu g\,L^{-1}$)
A[a]	1056	0.0–2.0	$y = -0.0984x + 0.7214$	0.9184	0.1098
A	1056	0.0–2.0	$y = -72.324x + 1047.3$	0.9428	0.0205
B[a]	2212	0.0–2.0	$y = -0.0985x + 0.7194$	0.9168	0.0514
B	2212	0.0–2.0	$y = -143.77x + 2195.6$	0.9481	0.0079
C[a]	5559	0.0–2.0	$y = -0.0984x + 0.7188$	0.9172	0.0030
C	5559	0.0–2.0	$y = -218.86x + 3531.7$	0.9524	0.0042
A[a]	1056	0.0–0.8	$y = -0.1683x + 0.7384$	0.9854	0.0642
A	1056	0.0–0.8	$y = -115.14x + 1057.8$	0.9915	0.0129
B[a]	2212	0.0–0.8	$y = -0.1689x + 0.7367$	0.9846	0.0533
B2	2212	0.0–0.8	$y = -224.92x + 2215.4$	0.9930	0.0050
C[a]	5559	0.0–0.8	$y = -0.1684x + 0.7359$	0.9833	0.0018
C2	5559	0.0–0.8	$y = -336.84x + 3560.5$	0.9933	0.0027
A[a]	1056	0.0–0.3	$y = -0.2226x + 0.7444$	0.9991	0.0485
A	1056	0.0–0.3	$y = -142.48x + 1060.8$	0.9964	0.0104
B[a]	2212	0.0–0.3	$y = -0.2244x + 0.7428$	0.9977	0.0401
B	2212	0.0–0.3	$y = -273.1x + 2220.7$	0.9965	0.0042
C[a]	5559	0.0–0.3	$y = -0.2269x + 0.7424$	0.9995	0.0013
C	5559	0.0–0.3	$y = -408.32x + 3568.3$	0.9976	0.0022

[a] This label indicates that linear regression was processed using absorbance as measurement parameter, and for the other ones were used potential deference variation according to Eq. (2).
[b] LD: limit of detection.

between intensity of the radiation beam falling on its observation window and the generated potential difference, thus a similar equation showed below was used to calculate the absorbance:

$$\text{Absorbance} = \text{Log}\left[\frac{\text{Sf}_i - \text{Sk}}{S - \text{Sk}}\right] \quad (1)$$

where Sk is the dark signal, Sfi is the reference signals of full scale ($I = 1, 2, 3$) and S is the read signal using a sample or standard solution.

In the dark condition that was achieved by tuning OFF the LED, the signal generated by the photometer should be different of 0 mV, thus it was included in the Eq. (1). Generally, its value was ≅2 mV.

The net variation of the electric potential difference, which is caused by the decrease of the radiation beam intensity when a radiation absorbing chemical specie is present into the flow cell, is represented by the following equation:

$$\text{SigVariation} = (\text{Sf}_i - \text{Sk}) - (S - \text{Sk}) \quad (2)$$

where symbols are as defined above.

Experimental data show that the net variation of the potential difference presented a linear relationship with analyte concentration. Based on the results, we observe that for microcystin screening methodology, this feature could be used as an alternative to absorbance. Aiming to prove the feasibility of this proposal, assays were carried out using both equations, and the results are shown in Table 2. For each full scale value, results were processed considering three ranges of microcystin concentrations. Analyzing the results, we can see that for absorbance, linearity characterized by R^2 was not affected when electric potential difference was set to 1056, 2067 and 3559 mV. Considering the Beer–Lambert law (Eq. (1)) this effect could be expected. The results obtained using the signal variation (Eq. (2)), afforded better linearity, as well as better limits of detection related to the two first cases, while for the reference measurement of 3559 mV similar values were achieved. These results show that variation of potential difference could be used for microcystin screening in water instead of using absorbance.

Usually for screening purpose there is a threshold concentration value and the monitoring setup must have sensitivity in order to detect the corresponding signal. In order to prove that the proposed setup could be used for this purpose, assays were carried out to achieve the signal variation using the blank measurement as a reference, yielding the results shown in Table 3. As we can see, the signals related to 0.05 $\mu g\,L^{-1}$ microcystins show that the proposed system afforded facilities for identifying this concentration level of microcystin, which is 20 times lower than the limit value established by the WHO [14]. These results show that a high value of full scale could be considered as a feasible resource, which could be employed to improve the screening ability of the propose procedure. The interface used to feed the blue LED allowed an easy adjustment of the radiation beam intensity emitted by the LED_1, hereby providing for ease use.

3.4. Sample analysis and results comparison

Sample preparation for microcystins determination followed the protocol recommended by the ELISA assay microplate kits manufacturer, as described in Section 2. Thus, after reaction development, the measurement was done using a photometer that directly read the signal in the wells. Afterwards, the samples were displaced from the wells to the flow cell of the proposed setup, and measurements were carried out. Considering the results shown in Table 2, a full scale value of 2200 mV was selected, and the results obtained are shown in Table 4. Applying the paired t-test at the 95% confidence level, the resulting value is 0.2395. The theoretical value is 0.81608, therefore, there is no significant difference between results. The detection limit of 0.03 $\mu g\,L^{-1}$ microcystin was estimated considering 3 times the standard deviation of the blank solution divided by the slope of the linear analytical curve that is the IUPAC recommendation [39]. Other profitable features such as a sample consumption of 60 μL per determination, and a waste generation of 100 μL per determination were also achieved.

Table 3
Effect of the full scale value on the signal variation.

Standard ($\mu g\,L^{-1}$)	Signal variation (mV)		
	A[a]	B[b]	C[c]
0.05	10.47 ± 0.72	20.66 ± 1.15	28.33 ± 3.79
0.10	11.78 ± 0.38	22.66 ± 1.53	35.00 ± 5.57
0.15	29.25 ± 0.26	57.66 ± 2.08	84.00 ± 5.57
0.30	41.88 ± 0.31	81.00 ± 2.52	121.33 ± 5.69
0.80	92.22 ± 0.06	180.00 ± 2.31	270.00 ± 6.08
2.00	147.55 ± 0.00	292.53 ± 3.02	445.67 ± 5.86

[a] Measurement achieved using full scale value of 1056 mV.
[b] Measurement achieved using full scale value of 2067 mV.
[c] Measurement achieved using full scale value of 3559 mV.

Table 4
Results comparison.

Microcystin concentration ($\mu g\,L^{-1}$)			
Sample	ELISA photometer	Proposed setup	
		Absorbance	Millivolt
1	0.71	0.73 ± 0.02	0.74 ± 0.01
2	0.00	0.08 ± 0.00	0.07 ± 0.00
3	0.08	0.07 ± 0.00	0.07 ± 0.00
4	0.17	0.19 ± 0.02	0.19 ± 0.00
5	0.20	0.24 ± 0.00	0.23 ± 0.00
6	1.54	1.46 ± 0.05	1.60 ± 0.05
7	0.00	0.05 ± 0.01	0.06 ± 0.00
8	1.20	0.88 ± 0.02	0.89 ± 0.00
9	0.11	0.19 ± 0.02	0.18 ± 0.00
10	0.20	0.24 ± 0.00	0.24 ± 0.01
11	0.08	0.09 ± 0.01	0.09 ± 0.00

Results average of three consecutive measurements.

Table 5
Performance comparison.

Concentration range ($\mu g\,L^{-1}$)	Linear coefficient (r^2)	Detection limit ($\mu g\,L^{-1}$)	Reference
0.05–2.00	0.999	0.03	Present paper
0.1–5.0	–	0.08	12
0.1–10	0.998	–	3
0.1–1.0	–	0.1	20
0.5–50	0.995	0.03	17
0.05–2.00	0.999	0.06	18

3.5. Performance comparison

Aiming to performance comparison with others existing methodologies for microcystin determination, linear response range and limit of detection were selected, which are summarized in Table 5. These data show that the comparison could be considered favorable to the proposed setup. Only Ref. [18] presented identical response, which was achieved using an expensive equipment setup.

3.6. Conclusion

The main goal to be attained in this work was microcystin screening in surface water at concentration levels lower than 1 $\mu g\,L^{-1}$, which is the WHO guideline value, using a small volume of sample solution. The objective was attained by combining a flow system of downsized dimension, a flow cell of long optical path length, and a dedicated control system that allowed an efficient handling of the sample solution.

The reduced volume of waste generated (100 μL per determination) allows us to conclude that the proposed setup satisfies the Analytical Green Chemistry requirement concerning environmental sustainability [35–37].

The flow cell shown in Fig. 1 was used for the first time in this work, which avoided retention of air bubble in the optical path, while allowing an improved coupling with radiation sources (LED_1, LED_2), thereby contributing to the success of the proposal.

Acknowledgements

Authors acknowledge the CNPq (G.P. Vieira graduate fellowship, proc. 130127/2008-6; M.F. Fiore, research fellowship, proc. 308299/2009-4, B.F. Reis, research fellowship, proc. 305043/2008-0), CAPES, FAPESP, PRONEX/FAPESB, and CNPq/INCTAA.

References

[1] M.E.V. Apeldoorn, H.P.V. Egmond, G.J.A. Speijers, G.J.I. Bakker, Review toxins of cyanobacteria, Mol. Nutr. Food Res. 51 (2007) 7–60.
[2] L. Spoof, M.R. Neffling, J. Meriluoto, Separation of microcystins and nodularins by ultra performance liquid chromatography, J. Chromatogr. B 877 (2009) 3822–3830.
[3] F. Gurbuz, J.S. Metcalf, A.G. Karahan, G.A. Codd, Analysis of dissolved microcystins in surface water samples from Kovada Lake, Turkey, Sci. Total. Environ. 407 (2009) 4038–4046.
[4] N. Khreich, P. Lamourette, A fluorescent immunochromatographic test using immunoliposomes for detecting microcystins and nodularins, Anal. Bioanal. Chem. 397 (2010) 1733–1742.
[5] G. Birungi, S.F.Y. Li, Determination of cyanobacterial cyclic peptide hepatotoxins in drinking water using CE, Electrophoresis 30 (2009) 2737–2742.
[6] T. Tsu tsu mi, S. Nagata, A. Hasegawa, Y. Ueno, Immunoaffinity column as clean-up tool for determination of trace amounts of microcystins in tap water, Food. Chem. Toxicol. 38 (2000) 593–597.
[7] E.D. Hilborn, W.W. Carmichael, M. Yuan, S.M.F.O. Azevedo, A simple colorimetric method to detect biological evidence of human exposure to microcystins, Toxicon 46 (2005) 218–221.
[8] S.M.F.O. Azevedo, W.W. Carmichael, E.M. Jochimsen, K.L. Rinehart, S. Lau, G.R. Shaw, G.K. Eaglesham, Human intoxication by microcystins during renal dialysis treatment in Caruaru, Brazil, Toxicology 181–182 (2002) 441–446.
[9] M.E. Silva-Stenico, R.C. Neto, I.R. Alves, L.A.B. Moraes, T.K. Shishido, M.F. Fiore, Hepatotoxin microcystin-LR extraction optimization, J. Braz. Chem. Soc. 20 (2009) 535–542.
[10] M.R. Neffling, L. Spoof, J. Meriluoto, Rapid LC–MS detection of cyanobacterial hepatotoxins microcystins and nodularins-comparison of columns, Anal. Chim. Acta 653 (2009) 234–241.
[11] P. Ferranti, S. Fabbrocino, A. Nasi, S. Caira, M. Bruno, L. Serpe, P. Gallo, Liquid chromatography coupled to quadruple time-of flight tandem mass spectrometry for microcystin analysis in freshwaters: method performances and characterisation of a novel variant of microcystin-RR, Rapid. Commun. Mass Spectrom. 23 (2009) 1328–1336.
[12] T. Triantis, K. Tsimeli, T. Kaloudis, N.T.E. Lytras, A. Hiskia, Development of an integrated laboratory system for the monitoring of cyanotoxins in surface and drinking waters, Toxicon 55 (2010) 979–989.
[13] D. Ortelli, P. Edder, E. Cognard, P. Jan, Fast screening and quantitation of microcystins in microalgae dietary supplement products and water by liquid chromatography coupled to time of flight mass spectrometry, Anal. Chim. Acta 617 (2008) 230–237.
[14] World Health Organization (WHO), Guidelines for Drinking Water Quality Addendum to Volume 2. Health Criteria and Other Supporting Information, 2nd ed., World Health Organisation, Geneva, 1998, pp. 95–110.
[15] T. Vinogradova, M. Danaher, A. Baxtera, M. Moloney, D. Victory, S.A. Haughey, Rapid surface plasmon resonance immunobiosensor assay for microcystin toxins in blue-green algae food supplements, Talanta 84 (2011) 638–643.
[16] X. Zhou, Y. Meng, H. Ma, G. Tao, Method for determination of microcystin-leucine-arginine in water samples based on the quenching of the fluorescence of bioconjugates between CdSe/CdS quantum dots and microcystin-leucine-arginine antibody, Microchim. Acta 173 (2011) 259–266.
[17] S. Pavagadhi, C. Basheer, R. Balasubramanian, Application of ionic-liquid supported cloud point extraction for the determination of microcystin-leucine-arginine in natural waters, Anal. Chim. Acta 686 (2011) 87–92.
[18] Y. Shan, X. Shi, A. Dou, C. Zou, H. He, Q. Yang, S. Zhao, X. Lu, G. Xu, A fully automated system with on-line microsolid-phase extraction combined with capillary liquid chromatography–tandem mass spectrometry for high throughput analysis of microcystins and nodularin-R in tap water and lake water, J. Chromatogr. 1218 (2011) 1743–1748.
[19] J. Rapala, K. Erkomaa, J. Kukkonen, K. Sivonen, K. Lahti, Detection of microcystins with protein phosphatase inhibition assay, high-performance liquid chromatography–UV detection and enzyme-linked immunosorbent assay comparison of methods, Anal. Chim. Acta 466 (2002) 213–231.
[20] T. Tsutsumi, S. nagata, F. Yoshida, Y. Ueno, Anti-idiotype monoclonal antibodies against anti-microcystin antibody and their use in enzyme immunoassay, Toxicon 36 (1998) 235–245.
[21] R.N.M.J. Páscoa, S.S.M.P. Vidigal, I.V. Tóth, A.O.S.S. Rangel, Sequential injection system for the enzymatic determination of ethanol in wine, J. Agric. Food Chem. 54 (2006) 19–23.
[22] A. Mimendia, A. Legin, A. Merkoçi, M. del Valle, Use of sequential injection analysis to construct a potentiometric electronic tongue: application to the multidetermination of heavy metals, Sens. Actuators B 146 (2010) 420–426.
[23] S. Vermeira, K. Beullensa, P. Mészárosa, E. Polshina, B.M. Nicolaïa, J. Lammertyna, Sequential injection ATR–FTIR spectroscopy for taste analysis in tomato, Sens. Actuators B 137 (2009) 715–721.
[24] M. Manera, M. Miró, J.M. Estela, V. Cerdà, Multi-syringe flow injection solid-phase extraction system for on-line simultaneous spectrophotometric determination of nitro-substituted phenol isomers, Anal. Chim. Acta 582 (2007) 41–49.
[25] F. Maya, J.M. Estela, V. Cerdà, Multisyringe flow injection technique as an effective tool for the development of greener spectroscopic analytical methodologies, Spectrosc. Lett. 42 (2009) 312–319.
[26] B.F. Reis, M.F. Giné, E.A.G. Zagatto, J.L.F.C. Lima, R.A. Lapa, Multicommutation in flow-analysis. Part 1. Binary sampling: concepts, instrumentation and

spectrophotometric determination of iron in plant digests, Anal. Chim. Acta 293 (1994) 129–138.
[27] B.F. Reis, A. Morales-Rubio, M. de la Guardia, Environmentally friendly analytical chemistry through automation: comparative study of strategies for carbaryl determination with p-aminophenol, Anal. Chim. Acta 392 (1999) 265–272.
[28] F.R.P. Rocha, P.B. Martelli, B.F. Reis, An improved flow system for spectrophotometric determination of anions exploiting multicommutation and multidetection, Anal. Chim. Acta 438 (2001) 11–19.
[29] M.B. Silva, S.S. Borges, S.R.W. Perdigão, B.F. Reis, Green chemistry-sensitive analytical procedure for photometric determination of orthophosphate in river and tap water by use of a simple LED-based photometer, Spectrosc. Lett. 42 (2009) 352–362.
[32] S.S. Borges, J.S. Peixoto, M.A. Feres, B.F. Reis, Downscaling a multicommuted flow injection analysis system for the photometric determination of iodate in table salt, Anal. Chim. Acta 668 (2010) 3–7.
[33] O.D. Leite, H.J. Vieira, O. Fatibello-Filho, F.R.P. Rocha, Multicommuted flow procedure for the determination of total and free cholesterol in eggs and human blood serum by chemiluminescence, J. Braz. Chem. Soc. 21 (2010) 1710–1717.
[34] M. Knochen, M. Pistón, L. Salvarrey, I. Dol, A multicommuted flow system for the determination of dextrose in parenteral and hemodialysis concentrate solutions, J. Pharm. Biomed. Anal. 37 (2005) 823–828.
[35] E. R-Torralba, F.R.P. Rocha, B.F. Reis, A. Morales-Rubio, M. de la Guardia, Evaluation of a multicommuted flow system for photometric environmental measurements, J. Autom. Method Manage. Chem. (2006) 20384.
[36] F.R.P. Rocha, J.A. Nóbrega, O. Fatibello-Filho, Flow analysis strategies to greener analytical chemistry. An overview, Green Chem. 3 (2001) 216–220.
[37] S. Garrigues, S. Armenta, M. de la Guardia, Green strategies for decontamination of analytical wastes, Trends Anal. Chem. 29 (2010) 592–601.
[38] K. Mitteilungen, A new conception of Bouguer–Lambert–Beer's law, Fresen. Z. Anal. Chem. 297 (1979) 419.
[39] G.L. Long, J.D. Winefordner, Limit of detection: a closer look at the IUPAC definition, Anal. Chem. 55 (1983) 712–714.

Biographies

Gláucia P. Vieira graduated in Industrial Chemistry from Methodist University of Piracicaba, Brazil (1996), and PhD in Chemical in Agriculture and Environmental Medium from University of Sao Paulo (Brazil) in 2009. Today has a position of Post-Doc researcher in the Center of Nuclear Energy in Agriculture of the University of Sao Paulo. The main interest includes development of analytical procedures environmentally friendly.

Sheila R.W. Perdigão has a technician position at the University of São Paulo since 1985, where its work includes technical support on the Laboratory of Analytical Chemistry.

Marli F. Fiore graduated in Biology from Methodist University of Piracicaba, Brazil (1980), and PhD in Microbial Biotechnology from University of Guelph, Canada (2000). She has a position of assistant professor at the University of Sao Paulo since 2001, where works on cyanobacteria systematic and cyanotoxins.

Boaventura F. Reis graduated in Physic from University Estadual Paulista (Brazil) in 1975, and PhD in analytical chemistry from University Estadual de Campinas (Brazil) in 1986. Today has the position of Full Professor of Analytical Chemistry of the University of Sao Paulo. The research interest includes flow injection analysis (FIA), multicommuted flow analysis (MCFA) and automated analytical procedures. The works published in the journals for analytical chemistry received more than 3700 citations.